

Research & Reviews: Journal of Engineering and Technology

A Thermodynamic Insight on Dissociation Pathways of Chlorinated Alkyl Sulfides: Computational Quantum

Gangadhar Andaluri*

Civil and Environmental Engineering, Temple University, Philadelphia, PA 19122, USA

Research Article

Received date: 24/03/2016

Accepted date: 07/07/2016

Published date: 17/07/2016

*For Correspondence

Gangadhar Andaluri, Civil and Environmental Engineering, Temple University, Philadelphia, PA 19122, USA

E-mail: gangadhar@temple.edu

Keywords: Computational quantum chemistry, Chlorinated alkyl sulfides, Energy diagrams, Dissociation pathways.

ABSTRACT

Organophosphorus compounds are widely used in the manufacturing industry and pyrolysis is most commonly used for their destruction. These compounds dissociate in to chlorinated alkyl sulfides and further dissociate in to toxic products. This study describes a computational approach to determine the pathways of dissociation of these compounds. Several pathways were examined and energy level diagrams were presented for each of the possible dissociation pathways. There is no information available on these pathways in literature and this study reduces the knowledge gap. Geometry optimizations were performed for the parent molecules, transition states and the dissociation products. This study suggested that using higher basis sets is better compared to using modest basis sets for energy calculations for chlorinated compounds.

INTRODUCTION

Several organophosphorus compounds are widely used during the industrial manufacturing processes, veterinary and human medicines and also during the manufacture of pesticides for agricultural purposes. These chemicals were also used to manufacture chemical warfare agents (CWAs)^[1-3]. These organophosphorus compounds such as sarin, mustard agent, VX nerve gases are lethal and highly toxic^[4,5]. These compounds were developed and used during the World Wars^[4,6-8]. Efforts are made worldwide to prevent the manufacture, usage and storage of these highly toxic compounds. However, a repeated use during several military conflicts and attacks shows that there is an imminent threat to the society and the environment^[7]. Intoxications have been reported worldwide due to the extensive use of these toxic chemicals^[5]. The decontamination of these compounds is of particular interest due to increased security concerns.

In general, the destruction of these chemical weapons is achieved heat, hydrolysis or by oxidation. The most commonly used technologies are (1) low-temperature low-pressure liquid phase detoxification; (2) low-temperature high-pressure liquid phase detoxification; (3) high-temperature pyrolysis; (4) moderate temperature high-pressure oxidation and (5) high-temperature low-pressure oxidation^[9]. Any building or a location that has been attacked with these CWAs, biological warfare agents (BWAs) or manufacturing toxic industrial chemicals (TICs) undergoes a decontamination process. However, this decontamination residue can still contain trace levels of toxic chemicals that may be adsorbed on to the building materials or personal protective equipment (PPE). In most of the cases, these residues are disposed off in high temperature, thermal incinerators or hazardous waste combustors.

During the hydrolysis, pyrolysis or oxidation processes, these toxic chemicals readily react with chlorine and form toxic byproducts such as chlorinated alkyl sulfides. For example, the thermal oxidation of mustard agent generates volatile organics such as vinyl chloride ($H_2C=CH-Cl$) and 2-chloroethanethiol ($HSCH_2CH_2Cl$)^[10]. Both these chemicals are highly toxic and considered as carcinogenic chemicals that fall under the highly flammable category. There are many studies that were conducted on the simulation of the destruction of these building materials and advanced computational models for the military incinerators^[11-14].

However, there are no studies on dissociation pathways of the toxic chlorinated alkyl sulfides that are formed during the destruction processes. This study deals with the computational quantum chemistry modeling for the dissociation pathways of chlorinated alkyl sulfides.

RESEARCH APPROACH

This study is mainly focused on the dissociation pathways of chlorinated alkyl sulfides ($\text{HSCH}_2\text{CH}_2\text{Cl}$, $\text{H}_2\text{CICSCH}_2\text{CH}_2\text{Cl}$ and $\text{H}_3\text{CSCH}_2\text{CH}_2\text{Cl}$). These compounds, the possible transition states and the products are calculated using computational methods in Gaussian G03-W suite for windows^[15,16]. The computational methods used in this study employed Gaussian G3B3 theory using B3LYP wave function theory with 6-31G (d) basis set and CBS-QB3 using B3LYP wave function theory with CBSB7 basis set for geometry optimization and frequency calculations. These methods were compared with Gaussian G3B3 and CBSQB3 theories using B3LYP wave function theory with 6-311 + G (2d, p) basis set for geometry optimization and frequency calculations. The dissociation pathways of the chlorinated alkyl sulfides are compared using these four different computational methods.

Gaussian-3 (G3) depends on the geometry optimizations obtained from second order perturbation model MP2/6-31G (d) and zero-point energies from Hartree-Fock model, HF/6-31G (d). Gaussian-G3B3 is a slight variation of the G3, where the geometry optimizations and zero-point energies are estimated using density functional theory B3LYP/6-31G (d). Using the G3B3 command for a molecule in the Gaussian suite, the following^[15,16] steps will be performed to calculate the energy:

- a. Geometry optimization
- b. Frequency calculations
- c. Single point energy calculations at the following levels
 1. QCISD(T)/6-31G (d)//B3LYP/6-31G (d) single point calculations
 2. MP4/6-31+G(d)//B3LYP/6-31G (d) single point calculations
 3. MP4/6-31G(2df, p)//B3LYP/6-31G (d) single point calculations
 4. MP2(Full)/G3Large//B3LYP/6-31G (d) single point calculations

The output file for a stable molecule specifies the temperature, pressure, zero-point correction (ZPE), Gaussian G3B3 energy at 0 K and 298 K, enthalpy, and free energy of the molecule. However, for a non-stable molecule such as transition states, it is essential to perform each step independently and compute the energy of the molecule as described in Equations 1 – 8^[15,16].

$$E_0(\text{G3B3}) = E[\text{MP4}/6\text{-}31\text{G}(\text{d})//\text{B3LYP}/6\text{-}31\text{G}(\text{d})] + \Delta E (+) + \Delta E (2\text{df}, \text{p}) + \Delta E (\text{QCI}) + \Delta E (\text{G3Large}) + \Delta E (\text{HLC}) + \Delta E (\text{ZPE}) + \Delta E (\text{SO}) \quad (1)$$

$$\Delta E (+) = E[\text{MP4}/6\text{-}31\text{+G}(\text{d})//\text{B3LYP}/6\text{-}31\text{G}(\text{d})] - E[\text{MP4}/6\text{-}31\text{G}(\text{d})//\text{B3LYP}/6\text{-}31\text{G}(\text{d})] \quad (2)$$

$$\Delta E (2\text{df}, \text{p}) = E[\text{MP4}/6\text{-}31\text{G}(2\text{df}, \text{p})//\text{B3LYP}/6\text{-}31\text{G}(\text{d})] - E[\text{MP4}/6\text{-}31\text{G}(\text{d})//\text{B3LYP}/6\text{-}31\text{G}(\text{d})] \quad (3)$$

$$\Delta E (\text{QCI}) = E[\text{QCISD}(\text{T})/6\text{-}31\text{G}(\text{d})//\text{B3LYP}/6\text{-}31\text{G}(\text{d})] - E[\text{MP4}/6\text{-}31\text{G}(\text{d})//\text{B3LYP}/6\text{-}31\text{G}(\text{d})] \quad (4)$$

$$\Delta E (\text{G3Large}) = E[\text{MP2}(\text{Full})/\text{G3Large}//\text{B3LYP}/6\text{-}31\text{G}(\text{d})] - E[\text{MP2}/6\text{-}31\text{G}(2\text{df}, \text{p})//\text{B3LYP}/6\text{-}31\text{G}(\text{d})] - E[\text{MP2}/6\text{-}31\text{+G}(\text{d})//\text{B3LYP}/6\text{-}31\text{G}(\text{d})] - E[\text{MP2}/6\text{-}31\text{G}(\text{d})//\text{B3LYP}/6\text{-}31\text{G}(\text{d})] \quad (5)$$

$$\Delta E (\text{HLC}) = -A * n_\beta - B * (n_\alpha - n_\beta) \quad (\text{molecules}) \quad (6)$$

$$= -C * n_\beta - D * (n_\alpha - n_\beta) \quad (\text{For atoms}) \quad (7)$$

$$\Delta E (\text{ZPE}) = 0.96 * \text{ZPE} [\text{B3LYP}/6\text{-}31\text{G} (\text{d})] \quad (8)$$

where, A = 6.760, B = 3.233, C = 6.786 and D = 1.269; n_α is the number of alpha valence electrons; n_β is the number of beta valence electrons. Complete basis set (CBS-Q3) methods were also used in this study for energy calculations. The CBS-Q3 theory is similar to G3 theory; however, the geometry optimizations and frequency calculations are performed using B3LYP wave function with a CBSB7 basis set. Single point energies were computed using the following levels and corresponding basis sets:

$$\text{a. CCSD}(\text{T})/6\text{-}31\text{G}(\text{d})//\text{B3LYP}/\text{CBSB7}$$

$$\text{b. MP4SDQ}/\text{CBSB4}//\text{B3LYP}/\text{CBSB7}$$

$$\text{c. MP2}/\text{CBSB3}//\text{B3LYP}/\text{CBSB7}$$

Similar to G3B3 energy estimations, the output file of a stable molecule specifies the temperature, pressure, zero-point correction (ZPE), Gaussian CBS-QB3 energy at 0K and 298K, enthalpy, and free energy of the molecule. However, the energy calculations for a transition state were calculated using Equations 9 – 17^[15,16].

$$E_0[\text{CBS}] = E[\text{HF}/\text{CBSB3}] + E [\text{ZPE}] + \Delta (\text{MP2}) + E2 [\text{CBS}] + \Delta (\text{MP3}) + \Delta (\text{CCSD}) + \Delta (\text{INT}) + \Delta (\text{EMP}) + \Delta (\text{SO}) \quad (9)$$

$$E [\text{ZPE}] = \text{ZPE} * 0.99 \quad (10)$$

$$\Delta (\text{MP2}) = E [\text{MP2/CBSB3}] - E [\text{HF/CBSB3}] \quad (11)$$

$$E2 [\text{CBS}] = E [\text{E2(CBS)/CBSB3}] - \Delta (\text{MP2}) \quad (12)$$

$$\Delta (\text{MP3}) = E [\text{MP4SDQ/CBSB4}] - E [\text{MP2/CBSB4}] \quad (13)$$

$$\Delta (\text{CCSD}) = E [\text{CCSD(T)/6-31+G(d`)}] - E [\text{MP4SDQ/6-31+G(d`)}] \quad (14)$$

$$\Delta (\text{INT}) = E [\text{CBS-INT}] - E [\text{E2(CBS)}] \quad (15)$$

$$\Delta (\text{EMP}) = 5.79 * O_{\text{iii}} / 1000 \quad (16)$$

$$\Delta (\text{SO}) = [\text{S}^2(\text{UHF}) - \text{S}^2(\text{Exact})] * 9.54 / 1000 \quad (17)$$

In this study, B3LYP wave function theory with 6-311 + G (2*d*,*p*) basis set for geometry optimization and frequency calculations were also used for energy calculations. Using a higher basis set allowed the addition of a diffuse and *d* function to the heavier atoms (Carbon, sulfur and chlorine) and *p* function to the hydrogen atoms.

RESULTS AND DISCUSSION

Figure 1 shows the structures of the compounds considered for this study and is drawn using Gauss-View (2000). The energy of the transition state molecules was calculated using the data from the output of the individual steps that were described above methods. Excel sheets were developed for the energy calculations using different computational methods. Considering thermal oxidation of $\text{H}_2\text{ClCSCH}_2\text{CH}_2\text{Cl}$, the following four dissociation pathways are possible:

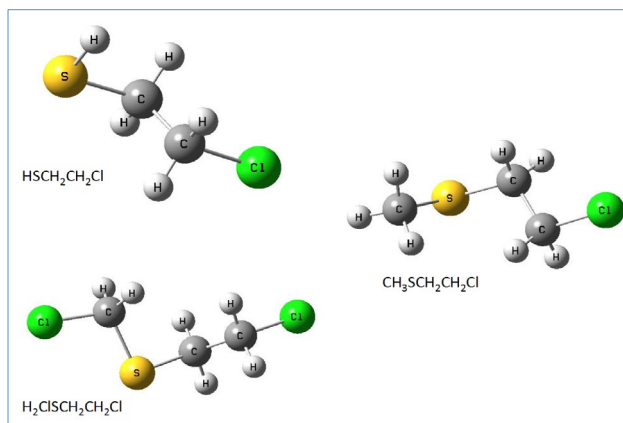


Figure 1. Chemical structure of Chlorinated alkyl sulfides considered for this study.

- HCl losses
- Bond breaks
- Ring eliminations and
- Retroene reactions

The HCl losses from C-1 and C-4 would result in the formation of $\text{CH}_2\text{ClSCH}_2\text{CH}$, HCl and $\text{CHSCH}_2\text{CH}_2\text{Cl}$, HCl. However, the α - β HCl losses from C-3 and C-4 would result in $\text{CH}_2\text{Cl-S-CH}_2=\text{CH}_2 + \text{HCl}$. **Figure 2** shows the dissociation structures of the products. Bond breaks can occur at C1 - S2, C3 - S2 or C3 - C4. These bond breaks will result in the formation of molecules shown in **Figure 3**. Ring eliminations of HCl can occur at C1 - C3 or C1 - C4 (**Figure 4**). Retroene reaction products are shown in **Figure 5**.

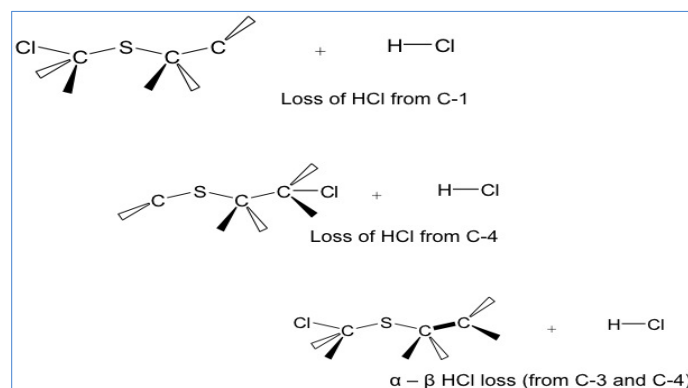


Figure 2. HCl losses from $\text{H}_2\text{ClCSCH}_2\text{CH}_2\text{Cl}$.

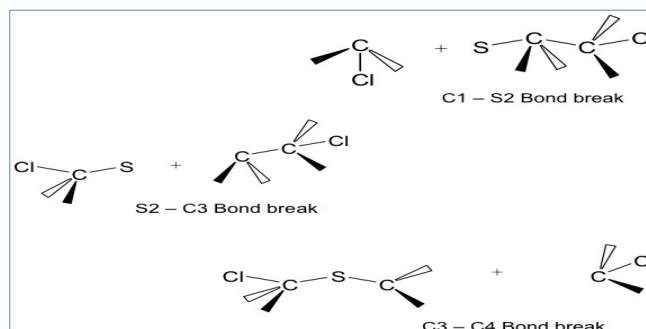


Figure 3. Possible bond breaks of $\text{H}_2\text{CICSCH}_2\text{CH}_2\text{Cl}$.

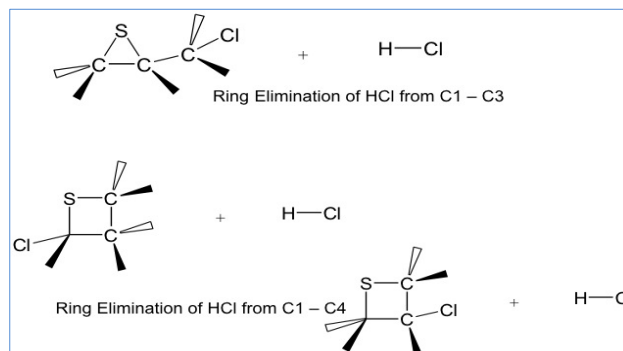


Figure 4. Ring eliminations of HCl from $\text{H}_2\text{CICSCH}_2\text{CH}_2\text{Cl}$.

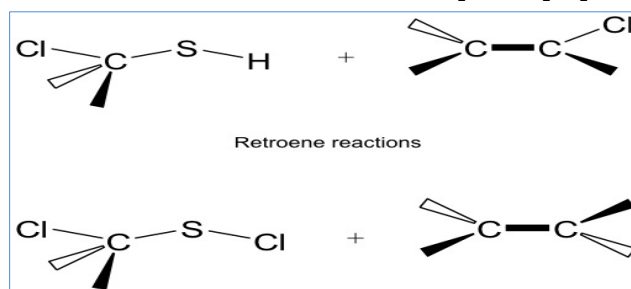


Figure 5. Retroene reactions of $\text{H}_2\text{CICSCH}_2\text{CH}_2\text{Cl}$.

The bond-breaking reactions during the oxidation process occur without the formation of any transition state molecules. However, the dissociation pathways such as retroene reactions, ring eliminations, and HCl losses could result in the formation of transition states. The retroene transition structures obtained during the computational modeling processes are shown in **Figure 6**. **Figure 7** shows the transition structures obtained during α - β HCl losses and **Figure 8** shows the ring elimination transition structures.

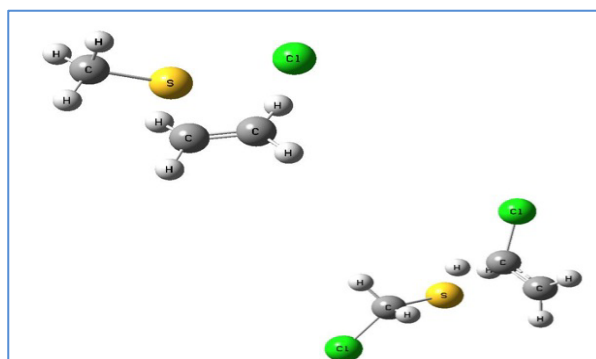


Figure 6. Transition structures for Retroene reactions of $\text{H}_2\text{CICSCH}_2\text{CH}_2\text{Cl}$.

These transition structures were also created in Gauss View and the geometry of the compounds were optimized using Gaussian G3B3 computational methods. The dissociation pathways of the other two compounds, $\text{H}_3\text{CSCH}_2\text{CH}_2\text{Cl}$ and $\text{HSCH}_2\text{CH}_2\text{Cl}$ are similar to the ones described for $\text{H}_2\text{CICSCH}_2\text{CH}_2\text{Cl}$ (not shown here). The energies of the compounds, transition structures and the reaction products were calculated using the four computational methods (G3B3/6-31G(d), G3B3/6-311+g(2d,p), CBS-QB3/CBSB7, and CBS-QB3/6-311+g(2d,p)) as described earlier. The calculated energies for the stable molecules, transition states and the reaction products are shown in supporting information (**Tables S1 and S2**). Energy diagrams were plotted for the dissociation pathways of

the molecules considered for the study. **Figures 9–14** show the energy level diagrams. Similar energy level diagrams were obtained in the experimental degradation studies conducted by Ritter et al. for thermal decomposition of chlorobenzenes^[17]. From the energy level diagrams, it can be observed that in most of the dissociations α - β HCl loss and 1-3 HCl to form ring compounds is favored rather than the ring formation and the retroene reactions. On an average, the retroene reactions require 10 – 25 kCal/mole higher energy compared to the HCl losses, ring eliminations and bond breaking steps. This supports the fact that most of the chemical dissociations requires higher temperatures for retroene reactions compared bond breaking reactions^[17,18].

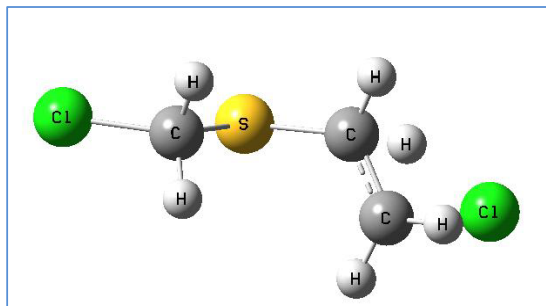


Figure 7. Transition structure of α - β HCl loses from $\text{H}_2\text{ClCSCH}_2\text{CH}_2\text{Cl}$.

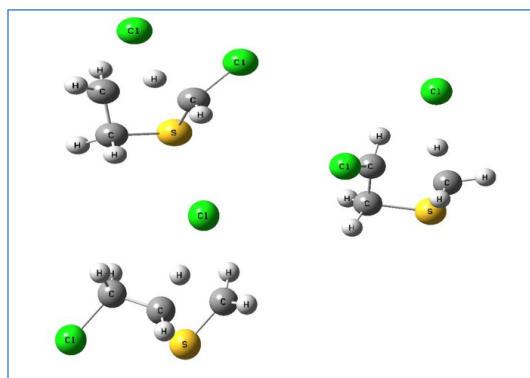


Figure 8. Transition structure for ring eliminations from $\text{H}_2\text{ClCSCH}_2\text{CH}_2\text{Cl}$.

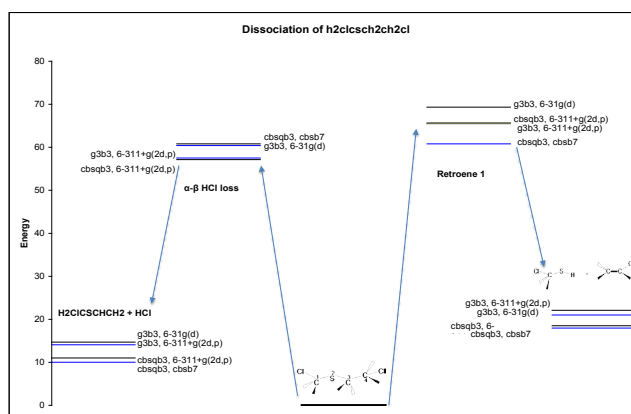


Figure 9. Energy level diagram for dissociation pathways of $\text{H}_2\text{ClCSCH}_2\text{CH}_2\text{Cl}$.

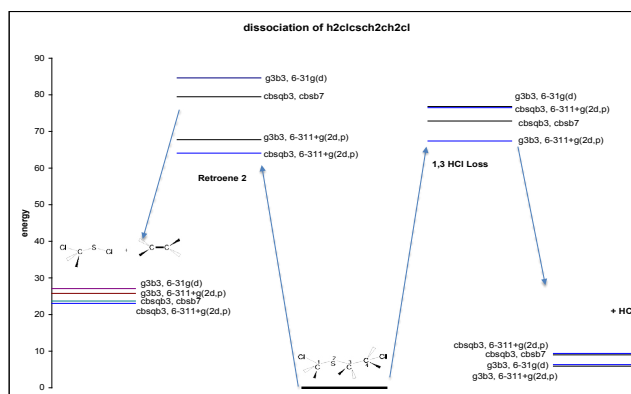


Figure 10. Energy level diagram for dissociation pathways of $\text{H}_2\text{ClCSCH}_2\text{CH}_2\text{Cl}$.

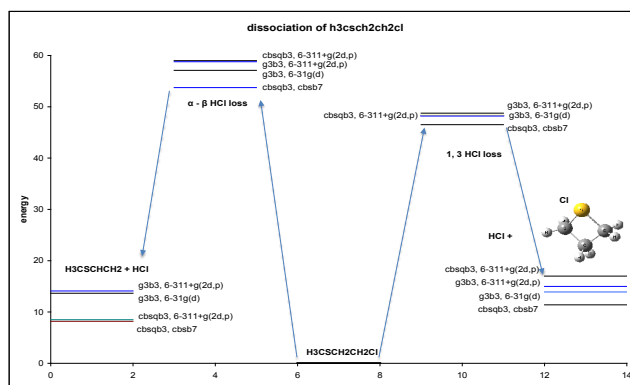


Figure 11. Energy level diagram for dissociation pathways of $\text{H}_3\text{CSCH}_2\text{CH}_2\text{Cl}$.

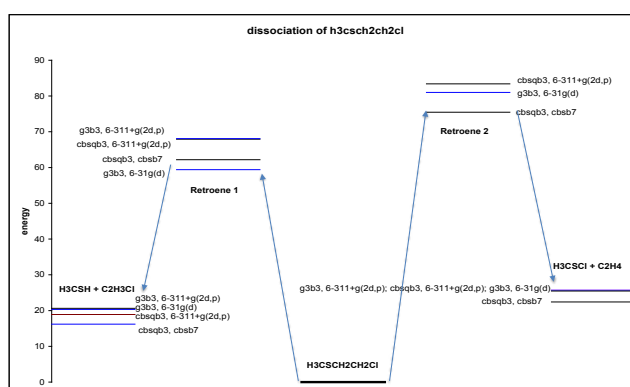


Figure 12. Energy level diagram for dissociation pathways of $\text{H}_3\text{CSCH}_2\text{CH}_2\text{Cl}$.

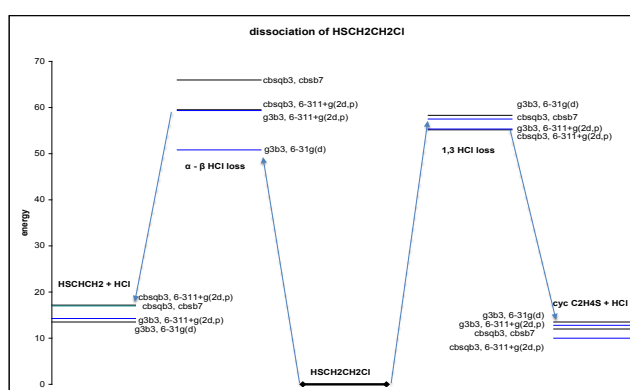


Figure 13. Energy level diagram for dissociation pathways of $\text{HSCH}_2\text{CH}_2\text{Cl}$.

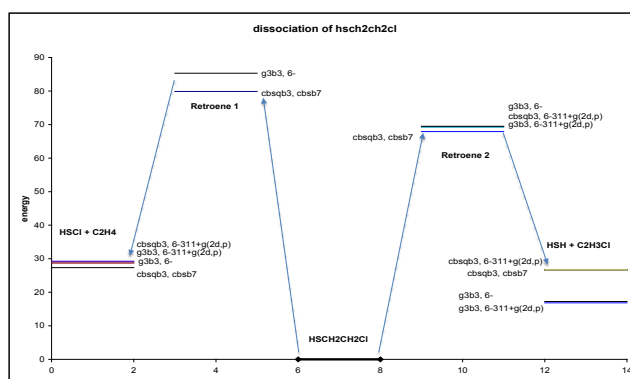


Figure 14. Energy level diagram for dissociation pathways of $\text{HSCH}_2\text{CH}_2\text{Cl}$.

It was observed that the energies calculated using G3B3 theory applying B3LYP wave function theory with a 6-31G(d) basis set were almost similar to those calculated using 6-311 + G (2d, p) basis set for stable molecules. For example, the energy of $\text{H}_3\text{CSCH}_2\text{CH}_2\text{Cl}$ calculated using G3B3/6-31G (d) and G3B3/6-311G (2d,p) were -612,770 and -612,771 kCal/mole, respectively. The average difference in the energy for a stable molecule and transition state were approximately 0.4 and 79 kCal/mole, respectively. However, energy estimated using CBS-QB3/CBSB7 and CBS-QB3/6-311G (2d,p) were 612,231 and 612,301

kCal/mole, respectively. The difference in the energies calculated CBS-QB3 theory was approximately 69 kCal/mole, which is significantly higher when compared to the G3B3 theory. The average difference in the energies calculated using CBS-QB3 theories for stable molecules and transition states was approximately 33 and 56 kCal/mole, respectively.

This suggests that using a modest basis set for the geometry optimization and frequency calculations may not be adequate and the use of higher basis set (i.e., addition of a diffuse function to heavier atoms) is suggested. Similar observations were made by Almlof et al. where using a higher basis sets for estimation of thermodynamic properties resulted in lower differences^[19].

CONCLUSIONS

This study was mainly focused on the computational quantum chemistry approach for the determining the dissociation pathways of chlorinated alkyl sulfides. Several reaction pathways were examined and the energy level diagrams are presented. Energy level diagrams showed that in most of the dissociations HCl losses are favored compared to the ring formation reactions and the retroene reactions. The calculations of the energies of these chlorinated alkyl sulfides showed an average difference for the calculations using 6-31G (*d*) and 6-311 + G (*2d,p*) basis sets for geometry optimization and frequency calculation for stable molecules to be around 0.8 kcal/mole and around 9 kcal/mole for transition state molecules. Experimental work on the dissociation of these molecules and analysis of the products on a GC/MS would provide more insights into these bond-breaking mechanisms.

ACKNOWLEDGEMENTS

Funding for this research was provided by Villanova University. Opinions, findings and conclusions expressed in this paper are those of the authors and do not necessarily reflect the views of Villanova University or Temple University.

REFERENCES

1. Macilwain C. Study proves Iraq used nerve gas. *Nature*. 1993;363:3.
2. Beesley WN. Sheep dipping, with special ref- erence to the UK. *Pesticides Outlook*. 1994;5:16-29.
3. Marrs TC. Toxicology of Organophosphate Nerve Agents in *Chemical Warfare Agents: Toxicology and Treatment*. John Wiley & Sons, Ltd. 2007.
4. Worek F, et al. Diagnostic aspects of organophosphate poisoning. *Toxicology*. 2005;214:182-9.
5. Singh R, et al. Detoxification of O,S-diethyl methyl phosphonothiolate, a simulant of VX, by N,N-dichlorourethane as an effective decontaminating agent. *Indian Journal of Chemistry*. 2011;50:1504-1509.
6. Schwenk M and Szinicz L. Chemical warfare agents--still taboo poisons? *Toxicology*. 2005;214:165-6.
7. Szinicz L. History of chemical and biological warfare agents. *Toxicology*. 2005;214:167-81.
8. Thiermann H, et al. Effects of oximes on muscle force and acetylcholinesterase activity in isolated mouse hemidiaphragms exposed to paraoxon. *Toxicology*. 2005;214:190-7.
9. National Research Council (U.S.). Committee on Alternative Chemical Demilitarization Technologies, et al. *Alternative technologies for the destruction of chemical agents and munitions*. Washington. DC: National Academy Press. 1993;16:323.
10. Martin KD, et al. Advanced Computational Modeling of Military Incinerators, in IT3'02 Conference. May, New Orleans, Louisiana. 2002.
11. Lemieux P. EPA Safe Buildings Program: Update on Building Decontamination Waste Disposal Area. *EM*. 2004;29-33.
12. Lemieux P. Pilot-Scale Combustion of Building Decontamination Residue in Air and Waste Management Association's 98th Annual Conference & Exhibition Minneapolis, MN. 2005.
13. Denison M, et al. Advanced Modeling of Incineration of Building Decontamination Residue, in Air and Waste Management Association's 98th Annual Conference & Exhibition Minneapolis, MN. 2005.
14. Lemieux P, et al. Thermal Destruction of Cb Contaminants Bound on Building Materials: Experiments and Modeling in Scientific Conference on Chemical and Biological Defense Research. Timonium, MD. 2005.
15. Ritter ER and Bozzelli JW. Kinetic study on thermal decomposition of chlorobenzene diluted in H₂, *Journal of Physical Chemistry*. 1990;94:2493-2504.
16. Moldoveanu SC. Pyrolysis of organic molecules with applications to health and environmental issues. *Techniques and Instrumentation in Analytical Chemistry*. 2010;28.
17. Almlof J, et al. Gaussian basis sets for High-Quality ab initio calculations, *Journal of Physical Chemistry*. 1988;92:3029-3033.
18. Moldoveanu SC. Pyrolysis of organic molecules with applications to health and environmental issues. *Techniques and Instrumentation in Analytical Chemistry*. 2010;28.
19. Almlof J, et al. Gaussian basis sets for High-Quality ab initio calculations. *The Journal of Physical Chemistry*. 1988;92:3029-3033.